Development of gallic acid-loaded ethylcellulose fibers as a potential wound dressing material

Alexa-Maria Croitoru, Musa Ayran, Eray Altan, Yasin Karacelebi, Songul Ulag, Ali Sahin, Mehmet Mucahit Guncu, Burak Aksu, Oguzhan Gunduz, Bianca-Maria Tihăuan, Denisa Ficai, Anton Ficai

PII: S0141-8130(23)03893-X

DOI: https://doi.org/10.1016/j.ijbiomac.2023.126996

Reference: BIOMAC 126996

To appear in: *International Journal of Biological Macromolecules*

Received date: 21 October 2022

Revised date: 12 September 2023

Accepted date: 17 September 2023

Please cite this article as: A.-M. Croitoru, M. Ayran, E. Altan, et al., Development of gallic acid-loaded ethylcellulose fibers as a potential wound dressing material, *International Journal of Biological Macromolecules* (2023), https://doi.org/10.1016/j.ijbiomac.2023.126996

Development of Gallic Acid-loaded ethylcellulose fibers as a potential wound dressing material

Alexa-Maria Croitoru[1,2,3], Musa Ayran[4], Eray Altan[5], Yasin Karacelebi[6], , Songul Ulag[6], Ali Sahin[7], Mehmet Mucahit Guncu[8], Burak Aksu[8], Oguzhan Gunduz[4,*], Bianca-Maria Tihăuan[1,9,10], Denisa Ficai[2,3], Anton Ficai[1-3,11,*]

[1]Department of Science and Engineering of Oxide Materials and Nanomaterials, Faculty of Chemical Engineering and Biotechnologies, University Politehnica of Bucharest, Gh. Polizu St. 1–7, 011061 Bucharest, Romania; alexa_maria.croitoru@upb.ro (A.-M.C.)
[2]National Centre for Micro- and Nanomaterials, University Politehnica of Bucharest, Spl. Independentei 313, 060042 Bucharest, Romania
[3]National Centre for Food Safety, University Politehnica of Bucharest, Spl. Independentei 313, 060042 Bucharest, Romania
[4]Marmara University, Center for Nanotechnology & Biomaterials Application and Research (NBUAM), Department of Metallurgical and Materials Engineering, Istanbul; ulagitu1773@gmail.com (S.U.)
[5]Faculty of Technology, Marmara University, Center for Nanotechnology & Biomaterials Application and Research (NBUAM), Department of Metallurgical and Materials Engineering, Istanbul; eray.altan@marmara.edu.tr (E.A.);
[6]Faculty of Engineering, Marmara University, Center for Nanotechnology & Biomaterials Application and Research (NBUAM), Department of Bioengineering, Istanbul; yasinkaracelebi@marun.edu.tr (Y.K.)
[7]Faculty of Medicine, Marmara University, Department of Biochemistry, Istanbul; alisahin@marmara.edu.tr (A.S.)
[8]Faculty of Medicine, Marmara University, Department of Medical Microbiology, Istanbul; mmguncu@gmail.com (M.M.G.)
[9]Research Institute of the University of Bucharest—ICUB, Spl. Independentei 91-95, 0500957 Bucharest, Romania
[10]Research & Development for Advanced Biotechnologies and Medical Devices, SC Sanimed International Impex SRL, 037040 Calugareni, Romania
[11]Academy of Romanian Scienusts, Ilfov St. 3, 050045 Bucharest, Romania
[*]Correspondence: oguzhan@marmara.edu.tr (O.G.); anton.ficai@upb.ro (A.F.)

Abstract

In this study, novel fibers were designed based on ethylcellulose (EC), loaded with different concentrations of gallic acid (GA) using the electrospinning technique, in order to investigate the potential of these materials as wound dressings. The chemical structure and morphology, along with the antimicrobial and biocompatibility tests of the EC_GA fibers were investigated. To observe the chemical interactions between the components, fourier transform infrared spectroscopy (FTIR) was used. The morphological analyzes were performed using scanning electron microscope (SEM). The uniaxial tensile test machine was used to obtain mechanical performance of the fibers. MTT assay was applied to get the biocompatibility properties of the fibers and antimicrobial test was applied to obtain the antimicrobial activity of the fibers. Based on the obtained results, the highest viability value of 67.4% was obtained for 10%EC_100GA on the third day of incubation, demonstrating that with the

addition of a higher concentration of GA, the cell viability increases. The antimicrobial tests, evaluated against *Staphylococcus* (S.) *aureus*, *Escherichia* (E.) *coli*, *Pseudomonas* (Ps.) *aeruginosa* and *Candida* (C.) *albicans*, showed a >90% microbial reduction capacity correlated with a logarithmic reduction ranging from 0.63 to 1, for 10%EC_100 GA. *In vitro* release tests of GA from the fibers showed that GA was totally released from 10%EC_100 GA fibers after 2880 minutes, demonstrating a controlled release profile. These findings demonstrated that EC_GA fibers may be suitable for application in biomedical fields such as wound dressing materials. However, further studies should be performed to increase the biocompatibility properties of the fibers.

Keywords: Electrospinning; ethylcellulose; fiber; gallic acid; tissue engineering; wound healing.

1. Introduction

In the biomedical domain, wound assesment and healing represent complex processes due to the many problems that can occure while treating acute and chronic wounds, such as: vascular disruption (1), local infections with germs (2), oxygenation, multiple comorbidities (3), obesity (4), diabetes, etc. (5, 6). Over the past years, due to technology's noteworthy progress, various bioactive dressings with improved properties were formulated to assist and improve the healing process of various wounds. These wound dressing materials should provide some important properties such as ensure bacterial protection, a moist environment, help accelerate re-epithelialization, transporting oxygen and nutrients and facilitating good cell adhesion. With their unique characteristics, polymeric materials are ideal candidates for designing scaffolds for wound dressing applications (7, 8, 9).

In the last decade, electrospun fibers have attracted a great deal of attention in wound healing applications, because of their outstanding architectural features (similar to the 3D structure of extracellular matrix), having a high surface to volume ratio, thus, being suitable for delivering various biological active agents to dermal cells, to tune the water and air permeation, to act as a barrier against microorganisms, etc. (10, 11).

EC is a water-insoluble etheric derivative of cellulose with numerous characteristics, such as excellent mechanical properties, barrier forming characteristics, high potential for use in drug delivery applications and excellent capacity to form films (12). EC is also a biodegradable and biocompatible polymer that has no toxicity and low production costs (13). Due to its unique features, EC can be used as support for wound dressings, having the potential to deliver the therapeutic agents (14, 15). EC was used in this study as carrier for the delivery of GA. In the literature data, GA is a phenolic agent reported as having antioxidant, antibacterial, anti-inflammatory, antitumoral and neuroprotective properties (16, 17, 18, 19, 20). Recent research has shown the potential of using EC as a material for wound dressing. For instance, Mohebian *et* al. (21) utilized the electrospinning technique to create

nanofibers composed of EC/hydroxypropyl methylcellulose that incorporated Aloe vera. The produced nanofibers demonstrated good biocompatibility, increased cell proliferation and adhesion and antibacterial activity against *Staphylococcus aureus* and *Escherichia coli* strains. Moreover, Wutticharoenmongko *et al.* (10) used the electrospinning technique to fabricate cellulose acetate (CA) nanofiber mats loaded with GA in different amounts. The release behavior of GA from the electrospun fibers was investigated in an acetate buffer solution (pH 5.5) and normal saline solution (pH 7.0). The maximum amount of released GA in acetate buffer solution was 97% and 71% for GACA 20wt.% and GACA 40 wt.%, while the maximum amount of released GA in normal saline was 96 and 81%, for GACA20wt.% and GACA 40 wt.%, respectively. The GA- loaded fibers also demonstrated antibacterial activity against *S. aureus*, demonstrating the potential for use as wound dressings. Li *et* al. (22) developed poly(vinylpyrrolidone) (PVP)/EC electrospun nanofibers loaded with ciprofloxacin (CIF), a model antibiotic, and investigated the morphological characteristics, *in vitro* drug release tests, and antibacterial assays in order to demonstrate the potential use of these electrospun materials in wound healing applications. The release behavior revealed a fast release of CIF from the PVP fibers and a much slower release from the EC fibers. Also, the nanofibers have been shown to possess antimicrobial properties, capable of inhibiting both Gram-positive and Gram-negative bacteria, due to the presence of CIF within the fibers.

The aim of the present paper was to fabricate 10%EC_GA fibers using the electrospinning technique and to investigate the potential of these materials as wound dressings. In this regard, surface morphology, mechanical and thermal properties, as well as the release profile, antimicrobial properties and cell viability tests were evaluated. This study focuses on the role of 10%EC_GA fibers as wound dressing materials, showing the promising future of biomedicine.

2. Materials and Methods

2.1. Materials

Chloroform and Tween 80 (viscous liquid) were purchased from Sigma-Aldrich, Taufkirchen, Germany, ethylcellulose 48.000 g/mol and gallic acid (≥98%) was purchased from Merck, Darmstadt, Germany.

2.2.Preparation of the electrospinning solution

A solution of 10% EC was obtained by dissolving the appropriate amount of EC (w/v) in 20 mL chloroform and stirring (at 300 rpm) for 2 hours at room temperature using a magnetic stirrer (Wise Stir®, MSH-20 A, Germany). After complete mixing, 3% Tween 80 was added in the 10%EC solution (w/v) and mixed for 15 minutes. The role of surfactant Tween 80 was to improve the stability of the electrospinning process and to reduce the surface tension of the electrospinning solution. Moreover, Tween 80 can increase hydrophilicity and promote the drug release from the fibers. Afterwards, different amounts of GA, 50, 75, and 100 mg (1%, 1.5%, and 2%) were added into the 10%EC

solution (w/v). The obtained solutions were mixed for one hour using the magnetic stirrer. The composition of solutions were given in Table 1.

Table 1. The composition of solutions.

Fibers	**EC** **% (w/v)**	**GA** **% (w/v)**	**Tween-80** **% (w/v)**
10%EC	10	-	3
10%EC_50 GA	10	1	3
10%EC_75 GA	10	1.5	3
10%EC_100 GA	10	2	3

2.3.Fabrication of the fiberss with the electrospinning method

Fibers were fabricated using an electrospinning machine (NS24, Inovenso Co., Turkey), connected to a syringe pump, (NE-300, New Era Pump Systems, Inc., USA). and a brass needle with an inner diameter of 1.63 mm. The voltaje varied between 24 kV and 26.5 kV, and the flow rate between 0.3 mL/h and 1 mL/h. The distance between the collector and the needle was set at 12 cm. The fibers were collected on a greaseproof paper that was covering the aluminium cylinder. The experiment was conducted in a 23 °C environment with a relative humidity of 50±3%. The schematic illustration of the electrospinning setup is given in Figure 1.

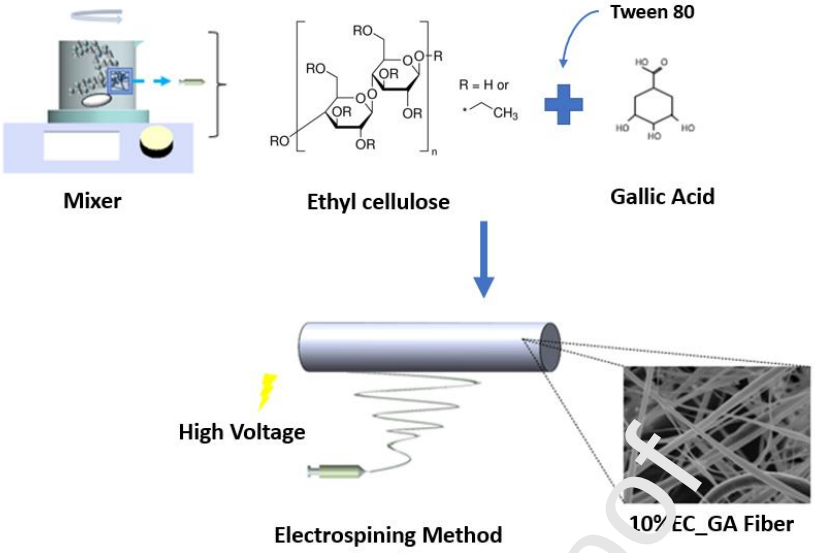

Figure 1. The schematic illustration of electrospining process.

2.4.Characterization of the fibers

The fourier transform infrared spectroscopy (FT-IR-4000, JASCO, Easton, MD, USA) with a scanning rate between 4000-400 cm^{-1}, was used to examine the chemical structure of the fibers. A total of 32 scans were performed with a resolution of 4 cm^{-1}. Know-it-all software was used to process the data and the test was carried out with one sample for each group.

The surface morphology of the fibers was investigated by scanning electron microscopy (SEM, MA-EVO 10, ZEISS, Munchen, Germany). Before the analysis, the fibers were coated with Au under vacuum for 60 s using a Quorum SC7620 Mini Sputter Coater. The mean diameter of the fibers was measured using the Olympus Analysis (USA) image software.

The mechanical properties were determined with the Shimadzu tensile test device (EZ-LX, Tokyo, Japan). The force value was adjusted to 0.1 N and the test speed value to 5 mm/min. The fibers were measured in triplicate, for all concentrations. The dimensions of all fibers were adjusted to be length: 50 mm, thickness: 0.2 mm, and width: 10 mm.

Differential scanning calorimeter device (DSC-6O Plus, Shimadzu, Japan) was used to investigate the thermal behavior of fibers consisting of 10%EC and GA. The samples were prepared by weighing precise amounts of fibers into a sealed aluminum pan with a lid that had a hole. The temperature was adjusted at 10 °C/min, while maintaining a nitrogen flow rate of 30–40 ml min^{-1}. The temperature was varied from -50 °C to 200 °C during the analysis.

2.5.In vitro drug release tests

The *in vitro* release tests of GA from fibers were determined in phosphate-buffered saline (PBS) solution, at pH 7.4 and a temperature of 37°C. The drug's linear calibration curve was determined in the wavelength range of 200-400 nm and for five distinct drug concentrations (0.2, 0.4, 0.6, 0.8 and 1 µg/mL). The first stage in the drug release test was to weigh 5 mg GA-loaded fibers and put them into Eppendorf tubes containing 1 mL PBS (pH 7.4). Afterwards, these tubes were put on the thermal shaker (BIOSAN TS-100C) at 37°C and 300 rpm to mimic the inside of the body. A quantity of 1 mL of each solution was collected at different time intervals (ranging between 0 and 48 hours) and analysed using an UV-Vis spectrophotometer (Shimadzu, Tokyo, Japan) in order to measure the amount of GA release into the PBS. After each measurement, new PBS was utilized at these time periods. The GA's release profile was monitored at 239 nm.

2.6.Antimicrobial susceptibility testing

Samples represented by 10%EC fibers loaded with GA were: 1) 10% EC, 2) 10%EC_50GA, 3) 10%EC_75GA, 4) 10%EC_100GA. We used as positive control for antimicrobial efficacy a 10 mg/mL GA solution. The negative control was represented by the untreated bacterial suspensions.

Assessment of antimicrobial efficacy was performed using four reference microorganisms by American Type Culture Collection (ATCC, Manassas, VA, USA): *Staphylococcus* (S.) *aureus* ATCC 6538, *Escherichia* (E.) *coli* ATCC 8739, *Pseudomonas* (Ps.) *aeruginosa* ATCC 9027 and *Candida* (C.) *albicans* ATCC 10231 and tree clinically acquired *S. aureus* strains (from wound infections – collection of Research Center of University of Bucharest). Microbial susceptibility was assessed according to CLSI 2019 M100 (23). Squares of 1 x 1 cm were cut from fibers and sterilised by exposure to UV light for 150 minutes on each side then incubated at 36 ± 2 °C for 4 hours with 1.5×10^8 CFU/mL microbial suspensions (standard density of 0.5 McFarland). After 4 hours of incubation, fibers were thoroughly spun on a vortex, and 6 decimal serial dilutions were carried out. 10 µL from each dilution were plated on solid Mueller Hinton agar, respectively Sabouraud for microfungi. After 24 hours of incubation plates were read by counting the colonies. Antimicrobial efficacy (AE) was expressed as logarithmic reduction using the formula: AE (CFU/mL) = lgA – lgB where A is CFU/mL of negative control (initial number of bacteria in the inoculum); B is CFU/mL of fibers (number of bacteria after x time of contact with antimicrobial substance). All tests were performed in triplicate.

The statistical analysis performed using GraphPad Prism 9 (San Diego, CA). Data were analyzed using the one-way ANOVA test. The level of significance was set to $p < 0.05$.

2.7.Biocompatibility tests

The L929 fibroblast cell line (ATCC, Manassas, CCL-1, Manassas, VA, USA) was utilized to evaluate the biological impact of the 10%EC_GA fibers. In standard humidity and temperature conditions (5 ± 1% CO_2, greter than 90% humidity and 37 ± 2 °C) , the cells were grown in Earle's

minimal essential medium (EMEM) containing L-glutamine (Biochrom, Merck Millipore, Darmstadt, Germany) and supplemented with 10% fetal bovine serum (FBS) and 1% penicillin and streptomycin antibiotics. UV irradiation sterilized the fibers for 30 mins on both sides. After sterilization, the scaffolds were subjected to overnight incubation with DMEM to enhance the scaffold surface properties, thereby promoting favorable cell attachment. The fibers for the cell test were prepared using a circular mold with a diameter of 5 mm and a thickness of 0.2 mm. Sterilized fiber structures were inserted in 96-well plates, and fibroblast cells (L929) were plated onto each fiber structure and cultured for one week under standard temperature and humidity conditions. All biological tests were repeated three times.

The MTT (3-(4,5-dimethylthiazol-2-yl)-2,5-diphenyl-2H-tetrazolium bromide) assay was used to quantify cellular viability and proliferation. At the appropriate time point, the media was gently withdrawn and replaced with fresh culture medium containing 10% MTT solution (5 mg/mL in PBS). The cells were cultured for another 3 hours under standard conditions before the supernatant was substituted with dimethyl sulfoxide (DMSO) to dissolve the extended formazan crystals. A microplate reader was used to determine the absorbance of each fiber at a wavelength of 570 nm.

Regarding the fluorescence microscopy morphological examination, 100.000 L929 cells in 400 µL culture media were planted onto each corresponding to 10%EC_GA fiber and allowed to adhere for 24 hours. Following this, the fibers were fixed for 10 minutes with 4% paraformaldehyde in PBS and marked for 10 minutes with 1 µg/mL DAPI (Invitrogen) in PBS. The images were taken with an Olympus BX-51 microscope configured with an Andor DSD2 Confocal Unit.

3. Results and Discussion

3.1.Morphological examination

Figure 2 shows the SEM images of the 10%EC and 10%EC_GA fibers. The fibers we obtained had a similar morphology and were arranged in a network of beads, although there was some variability in their size. The formation of beads might be due to the EC concentration, viscosity and evaporation rate of solution. A low concentration of 10%EC/chloroform solution might not assure sufficient viscosity, allowing the solution jet to form spherical shapes under the surface tension force. Figure 2 also presents the size distrubution of 10%EC, 10%EC_50GA , 10%EC_75GA, and 10%EC_100GA fibers with a diameter of 1.65 ± 0.326, 1.72 ± 0.467, 1.56 ± 0.368, and 1.63 ± 0.339 µm, respectively. The obtained fibers have a microfiber structure, according to these findings. The fiber structure is both randomly oriented and continuous, with small variations in size, which appear to spread more with the addition of GA.

With the addition of 50 mg of GA into the 10% EC fibers, the diameters of the fibers increased to 1.72 ± 0.467 µm (Figure 2b). By adding 75 mg of GA, the diameter of the fibers lightly decreased to 1.56 ± 0.368 µm (Figure 2c). ~~The decrease in fiber diameter with an increase in gallic~~

~~acid content can be attributed to the corresponding increase in solution conductivity, which enables the generation of elongation forces and results in the production of narrower fibers. This decrease in fiber diameter is mainly attributed to the presence of gallic acid. The higher electrical conductivity values result in increased elongation of the jet and formation of fibers with smaller diameters, while lower conductivity levels lead to insufficient elongation of the jet and the formation of bead-like structures, under identical processing conditions. Consistent with this notion, an elevation in the concentration of GA leads to an augmentation in the occurrence of bead structures as revealed by the SEM images as it can result in poor mechanical properties.~~ Overall, it can be concluded that adding different ratios of GA to the 10%EC fibers did not cause significant differencies between the diameters of the fibers. These results demonstrate that 10% EC fibers are compatible with GA and can be loaded with it without significantly affecting their fiber diameter, indicating that the as-loaded GA was well incorporated within the 10%EC fibers.

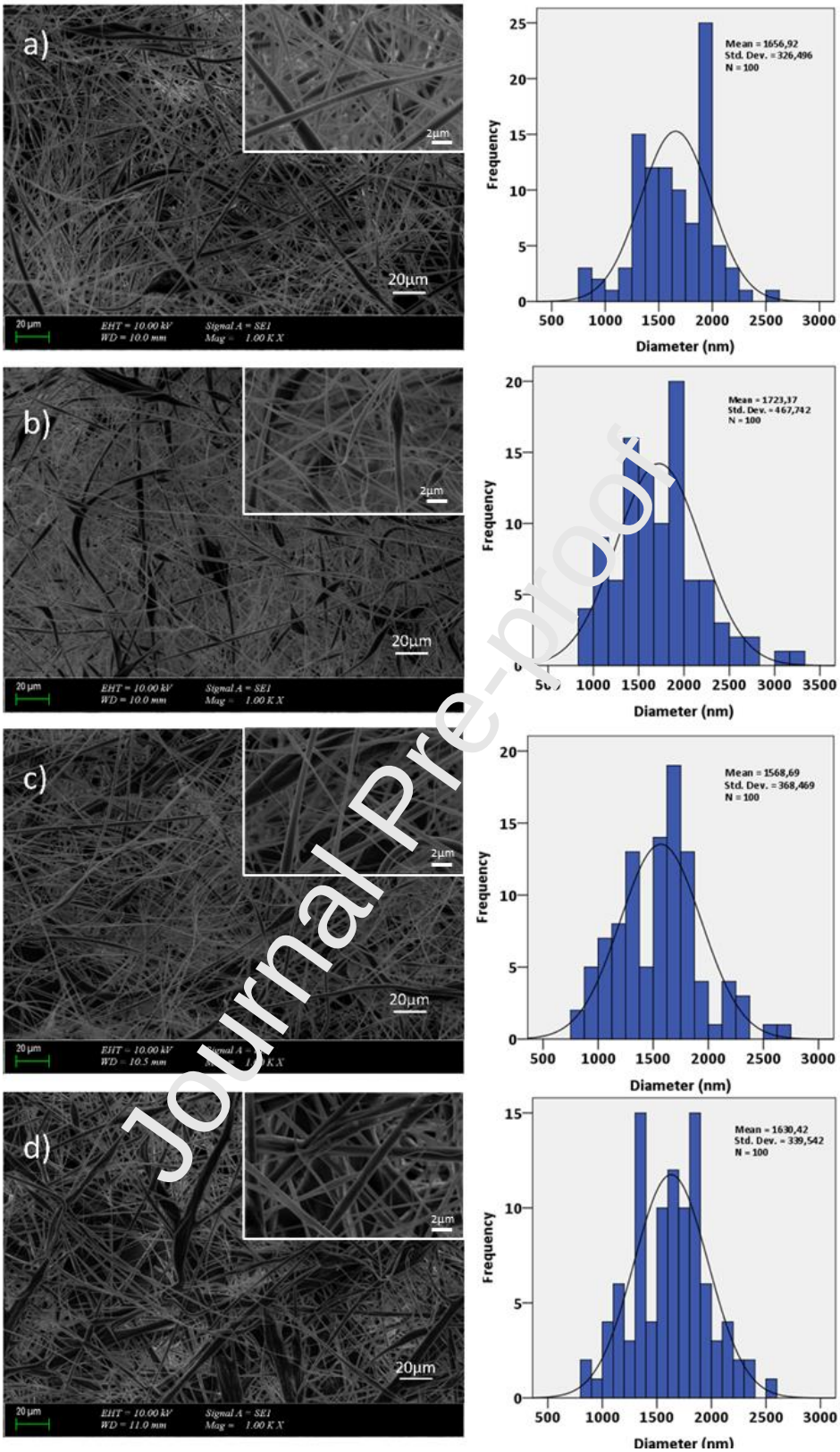

Figure 2. SEM images of the 10%EC (a), 10%EC_50GA (b), 10%EC_75GA (c), and 10%EC_100GA (d) and their diameter distribution.

3.2.FTIR analysis

FTIR analysis (shown in Figure 3) was performed to specify the main chemical groups of 10%EC, GA and 10%EC_GA fibers. The main characteristic peaks of 10%EC fibers observed at 3500 cm^{-1} (−OH stretching), and 1300 cm^{-1} (–CH_2 bending), respectively, are shown in Figure 3b. The peak from 1050 cm^{-1} and the band between 2870 and 2974 cm^{-1} is attributed to –C–O–C– stretching in the cyclic ether and the –CH_3 stretching vibration, respectively (24).

The characteristic peaks of GA (Figure 3a) at 3500 cm^{-1} and 3250 cm^{-1} correspond to the stretching modes of the different O–H groups. The stretching and bending vibrations of C=C bonds of aromatic ring and carboxyl groups, are mainly characterized by bands in the 1606–1381 cm^{-1} region. The bending vibrations of the C–H bonds in the ring structure and O–H of the phenol alcohol occurs arround 730 cm^{-1} and at 1174 cm^{-1} respectively. The stretching and bending vibrations of the C–O groups is shown at 1021 cm^{-1} for GA (25). After the loading of GA onto 10%EC fibers, the FTIR spectrum showed no significant changes, however some of these bands being overlapped, instead of individual peaks a composed peak can be observed, and thus, the intensity is proportional with the sum of the individual peaks. By adding GA into the 10%EC fibers, the peak that is characteristic of GA can be observed at ~1350 cm^{-1} which demonstrates the interaction of GA with 10%EC. Also. an increase in the relative intensity of the band between 2870 and 2974 cm^{-1} can be observed due to the increase in the GA concentration, highlighting the interaction of the GA with the EC.

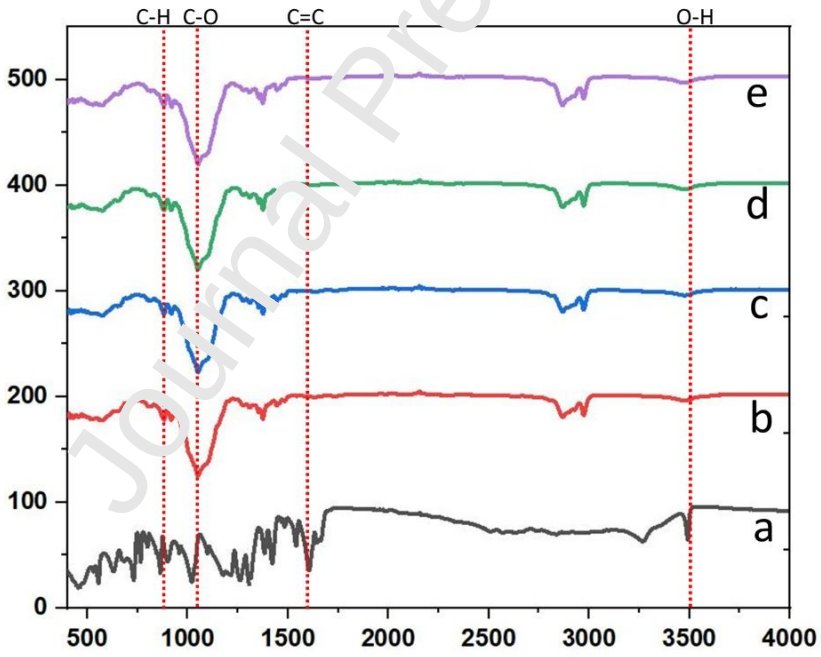

Figure 3. FTIR spectrums of the GA (a), 10%EC (b), 10%EC_50GA (c), 10%EC_75GA (d), and 10%EC_100GA (e).

3.3.Thermal analysis of the fibers

DSC is used to detect drug-excipient compatibility to provide maximum information regarding the possible interactions. The thermal behavior of GA and 10%EC_GA fibers were evaluated and is presented in Figure 4.

Pure GA exhibited a strong endothermic peak at 264 °C, which is related to the melting temperature of the crystal form of GA, which is a value close to the studies reported by Singh et al. (26) and Olga et al. (27). Furthermore, the 10%EC fiber exhibited a strong exothermic peak at 199 °C and another exothermic peak near 352 °C, which were shown to be connected to the crystallization temperature of of 10%EC fiber, and to thermal degradation of 10%EC (decomposition of the polymer), respectively (28). Moreover, the observation of the vanishing of the distinctive melting endothermic peak at 264°C in GA and the concomitant upward shift of the peak in 10%EC from 199°C to 243°C may provide compelling evidence for the formation of the complex. In this case, the formation of hydrogen bonds could lead to changes in the intermolecular interactions between GA and 10%EC fibers, affecting its thermal properties (29, 30). This also may have caused a change in the local environment of the GA molecules, leading to disappearance of the Tm point. The lack of a distinct glass transition temperature (T_g) peak of all fibers may be attributed to the formation of a complex or an intermolecular interaction, which has potentially altered the thermal properties of the system. This alteration of the molecular dynamics and the potential formation of new supramolecular structures may have hindered the observation of a clear T_g peak in the DSC analysis.

Figure 4. DSC curves of the pristine GA and 10%EC_GA fibers.

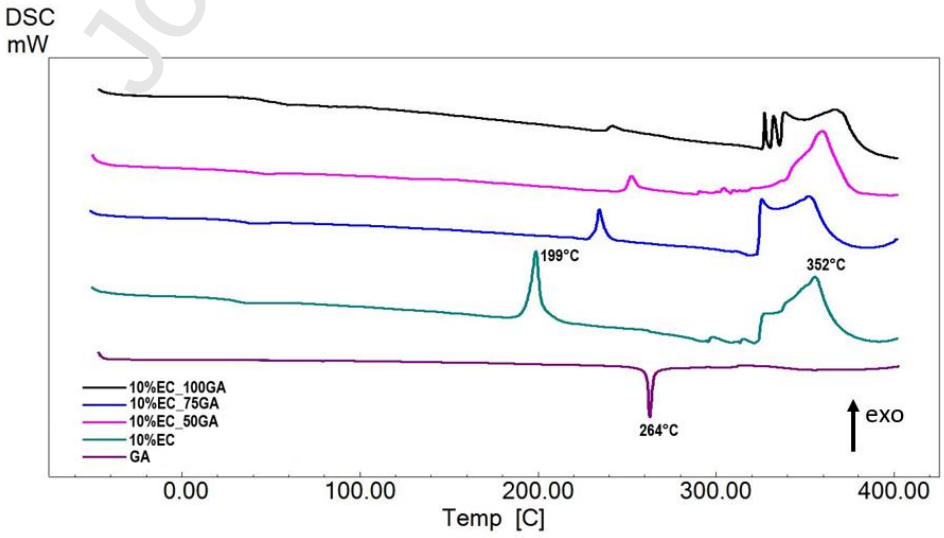

3.4.*Tensile behavior of the fibers*

Tensile stress values of 10%EC and GA-loaded fibers are shown in Table 1. The tensile test value for 10%EC was found to be 0.42±0.03 MPa and the strain value was found to be 1.30±0.77%. By addition of 50 mg of GA into the 10%EC, the average tensile stress values decreased to 0.33±0.01 Mpa and also the average strain value decreased to 0.98±0.34%. Compared to 10% EC_50GA, both tensile strength (0.34±0.08 Mpa) and strain value (1.00±0.42%) of 10%EC_75GA was mildly increased. The highest tensile strain value was found in 10%EC_100GA (0.42±0.03 Mpa). It can be concluded that adding GA to 10%EC_GA fibers did not significantly impact their tensile strength, which may be related to the usage of low GA concentration. However, adding GA to 10%EC resulted in reduced strength and less elasticity. A similar pattern of results was obtained in the research for wound dressing where the increase in the GA content showed a decrease in strength of the fibers (10). The underlying mechanism responsible for the reduction in mechanical strength is attributed to the disruptive effect of GA on the packing and alignment of the EC polymer chains. This can be hypothesized to be caused by the possible establishment of hydrogen bonds between GA and the EC fibers, resulting in the interference of intermolecular forces that govern the structural integrity of the EC fibers. Upon comparison of the results obtained for the fibers with those of commercially available wound dressings, it was observed that the mechanical strength fell within a similar range. Moreover, the observed values for elongation in the fibers under examination were determined to be lower in comparison to those of commercially available products, which suggests an increase in stiffness (31).

Table 1. Tensile testing results of the fibers.

Fibers	Tensile strength (Mpa)	Strain at Break (%)
10%EC	0.42±0.03	1.30±0.77
10%EC_50GA	0.33±0.01	0.98±0.34
10%EC_75GA	0.34±0.08	1.00±0.42
10%EC_100GA	0.35±0.17	1.15±0.40

3.5.Antimicrobial activity assesment

Skin can be damaged by a plethora of physical and chemical agents, at various degrees, with thermal, mechanical, and radial factors, or as a result of the reactions they create. Extending far down, exposed subcutaneous tissue brings forth a favorable microenvironment that is targeted by a wide variety of microorganisms with contamination and colonization outcome. Moreover, if the involved tissue is devitalized (e.g., ischemic, hypoxic, or necrotic) and the host immune response is

compromised, the conditions become ideal for microbial growth and proliferation. Therefore, our evaluation of the antimicrobial efficiency of fibers was performed on microbial strains with documented harmful impact on patients, especially hospitalized ones or with open wounds (32, 33, 34, 35).

A valuable tool used in determining the balance between efficacy and safety in this case relies on methods for assessing antimicrobial activity and adherence. These are carried out in order to establish the safety of the biomedical use of the materials or to verify the efficiency of their use in limiting infections or during decontamination processes. Medical devices that incorporate agents or materials with an antimicrobial effect are characterized by the ability to significantly limit, or even suppress, the development of microorganisms on their surface and/or in their volume, under suitable conditions of temperature, the composition of the gaseous environment, and nutrient supply. Their propagated antimicrobial activity is also dependent on the diameter of the fibers, the hydrophilicity of the surface, and their roughness and stiffness, all aspects must be taken into account, aspects known to have a direct correlation in affecting the ability of bacteria to attach and proliferate within the fibrous networks. Percentage microbial reductions of more than 90% are considered optimal for the intended application, provided that the biocompatibility of the fibers in question is certain.

In this study, it was observed that the bioactive fibers based on 10%EC_GA fibers, representing the main antimicrobial active, at different concentrations, yielded various rates of microbial reduction, most of them being considered highly effective. 10%EC fiber presented the lowest antimicrobial effect (Figure 5). These results were expected, as the support material alone does not have a significant antimicrobial effect, but other research has shown that EC functionalized with other materials that lead to the development of electrospun fibers demonstrated antimicrobial and antioxidant properties (36).

GA, as known from the literature, is a hydroxybenzoic acid with a strong antibacterial effect (37, 38, 39) on Gram-negative and Gram-positive bacteria (40) and an equally potent antifungal effect (41). Its action relies on induction of irreversible changes in microbial fiber properties. Therefore, in our study we observed that increased GA concentrations provide better antimicrobial effect, and proper active release from 10%EC fibers.

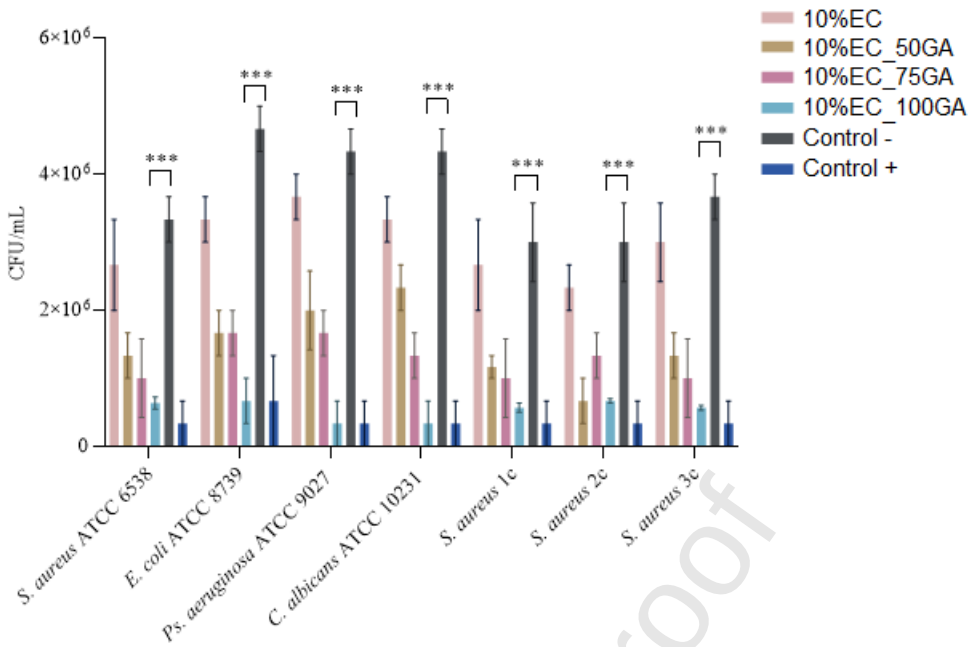

Figure 5. Antimicrobial efficacy of fibers 1) 10% EC, 2) 10%EC_50GA, 3)10%EC_75GA, 4) 10%EC_100 GA, as CFU/mL reduction. Positive control = 10 mg/ mL gallic acid solution. Negative control = untreated bacterial suspensions. *** *p value* < 0.003.

10%EC_100 GA fiber presented the highest efficiency on all tested strains, standardized as well as clinically acquired ones (from infected wounds), with logarithmic reductions (Figure 6) ranging from 0.63 to 1. This reduction level signifies an over 90% efficacy in microbial reduction. Following as level of effect was 10%EC_75GA fiber with logarithmic reduction ranging from 0.3 to 0.7. Both fibers presented outcomes similar to the positive control (control +) represented by a GA solution of 10 mg/mL.

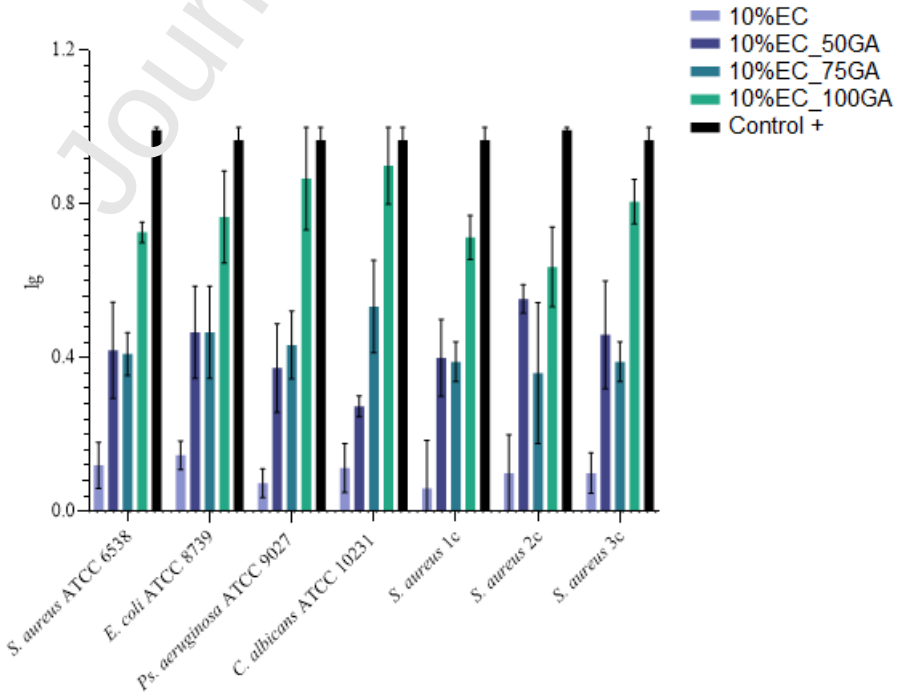

Figure 6. Antimicrobial efficacy expressed as logarithmic reduction (lg) for fibers 1) 10% EC, 2) 10%EC_50GA, 3)10%EC_75GA, 4) 10%EC_100 GA, as CFU/ml reduction. Positive control = 10 mg/ mL GA solution.

One of the main functions of wound healing medical devices is to provide proper support (pharmacological and physiological) to the affected site until the systemic treatment kicks in, therefore it is important that the embedded actives have the ability to promote adequate bacterial management. On this note, the action of GA on altering microbial cell membranes by disrupting their integrity has been reported (42, 43, 44). Compromised permeability of Gram-positive and Gram-negative bacterial membranes leads to higher accumulation rates of antibiotics, resulting in a direct synergistic effect between onsite treatment and systemic pharmacological intervention. The antioxidant effect as well as the promotion of wound healing have been reported as effects mediated by GA (45). Keeping in mind that biocompatibility is key, several articles present GA selective cytotoxicity pattern (46, 47, 48), indicating its potential use as an antitumoral agent, and reported good proliferation rate on keratinocytes and fibroblasts (45).

Overall, it can be concluded that the incorporation of 10%EC_100 GA fiber has great potential in enhancing the antimicrobial activity against both gram-negative and gram-positive bacteria. The results indicate that the CFU/mL count for both types of bacteria was significantly reduced with increasing concentrations of 10%EC_100 GA fiber. The log graph shows a dose-dependent decrease in bacterial growth, with the greatest reduction observed at the highest concentration of 10%EC_100 GA fiber. These findings suggest that the use of 10%EC_100 GA could be a promising approach for the development of antibacterial materials, especially for wound dressings and other biomedical applications.

3.6. Biocompatibility properties of the fibers

L929 fibroblast cells were used in order to determine the cytocompatibility of 10%EC and 10%EC_GA fibers. Cell viability results are presented in Figure 7. The results were calculated as percentage of untreated control 2D (fibroblast cell line), to which was attributed the value of 100%. The cells treated with 10%EC extract showed a similar behavior after 1, 3 and 7 days of incubation, revealing a slightly cytotoxic effect in L929 cells with a viability of about 70%. On the contrary, 10%EC_50GA induced a statistically significant cytotoxic response of fibroblasts for all time intervals, when the viability decreased with more than 50%, compared to the control. The highest cell viability and proliferation (67.4%) was obtained for fibroblast cells at 3 days after interaction with 10%EC_100GA fiber. This results can be attributed to the increase of GA content in the fibers that lead to an increase in the cell viability and cell proliferation of the GA-loaded fibers. Although, the loading of the drug initialy decreased the viability and proliferation of the fibroblast cells, with the adition of a higher concentration of GA, an increase in cell viability can be observed (22, 49).

Therefore, it is necessary to conduct additional research in order to optimise the fabrication conditions in order to increase the cell viability and proliferation of the fibers.

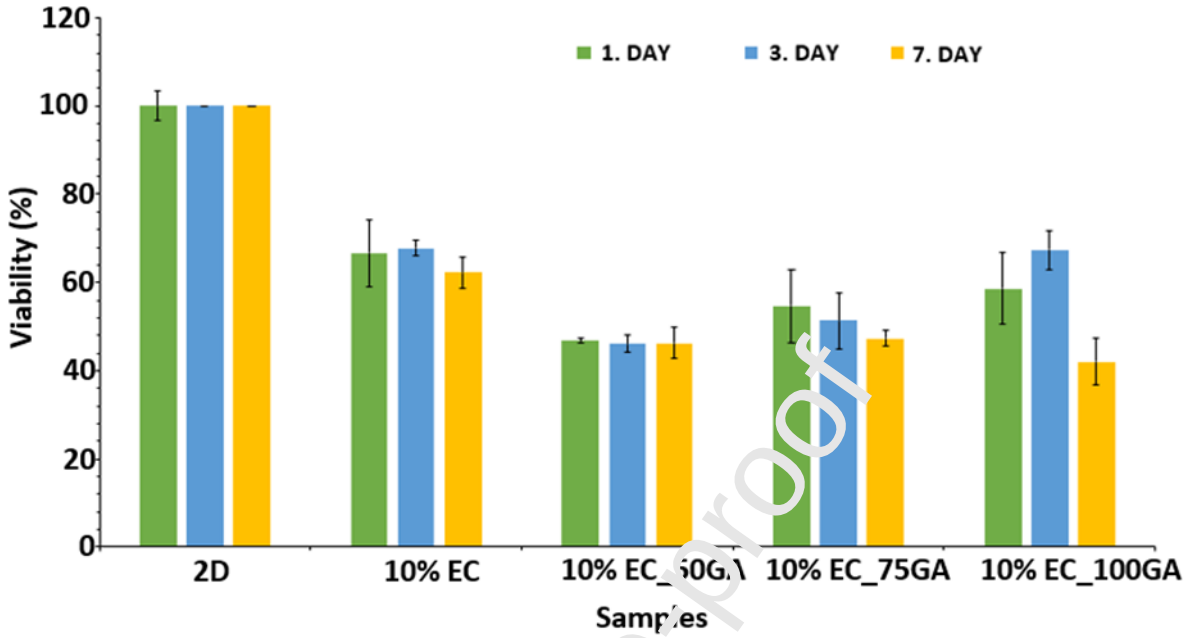

Figure 7. MTT viability for L929 fibroblast cells cultivated on the 10%EC fibers at different time intervals: 1.Day, 3 Days and 7 Days, respectively; data are expressed as mean ±SD. Comparison to 2D, ***p<0,001

Fluorescence microscopy of the fibroblast cells was examined to show the morphology of the L929 cells cultured on the fibers (Figure 8). The images show that the cells exposed to the fibers have similar morphology to the control and do attach to the 10%EC_GA fibers (50). It was observed that the cells on the GA-loaded fibers supported proliferation by forming clusters. The fibers in which the intensity is seen most by forming clusters were observed in 10%EC_50GA, and 10%EC_75GA fibers.

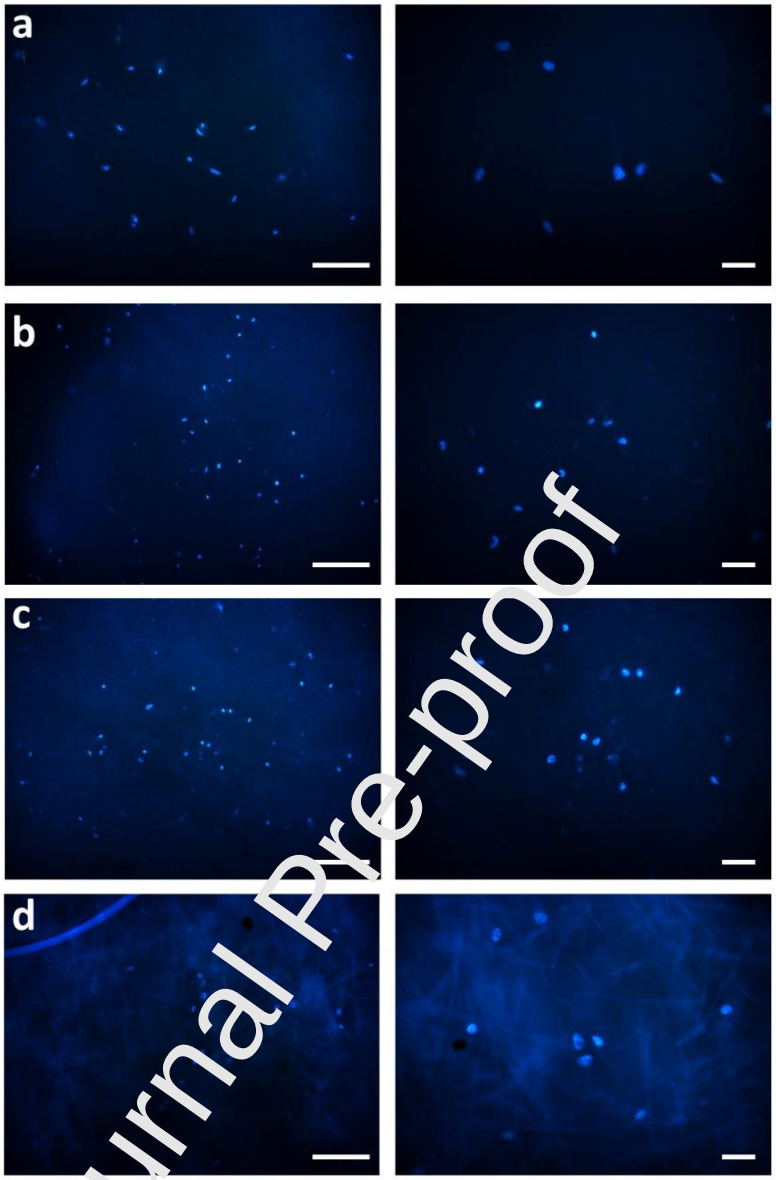

Figure 8. Fibroblast cell distributions on the fibers; 10%EC (a), 10%EC_50GA (b), 10%EC_75GA (c), and 10%EC_100GA (d).

3.7. In Vitro drug release

The drug release characteristics of GA-loaded fibers were investigated. The drug's calibration curve was established using five different concentrations (ranging from 0.2 to 1 g/mL), and the graph is shown in Figure 9. (A). Figure 9. (B) depicts the absorbance of the GA at 239 nm. *In vitro* release profile of GA from fibers in PBS medium was examined at room temperature, as depicted in Fig. 9.(C). In the first 3 hours, 41.92, 51.86, and 62.22% of GA was released from the 10%EC_50GA, 10%EC_75GA, and %10EC_100GA, respectively. At 24h, the greatest levels of GA released from 10%EC_100GA were approximately 87%. GA was totally released from of fibers after 48h.

The quantity of GA released from 10%EC_100GA fiber in PBS buffer was higher than that from the other fibers and this can be explained by mass transfer principle. Higher quantities if GA can enable more diffusion of drug molecules into the medium (10, 51). . According to the previous research, GA was loaded into mesoporous silica and found that it can released quite fast, 80-90% being released within 1/2h (52). These membranes released the GA quite quickly and it was expected that the drug delivery rate can be further tuned by loading more GA into the materials. Comparing with these results it is evident that the prolonged drug delivery provided by 10%EC_GA fibers can be advantageous for efficient drug release at the wound site and also can prevent the treatment from being rapidly removed from the wound.

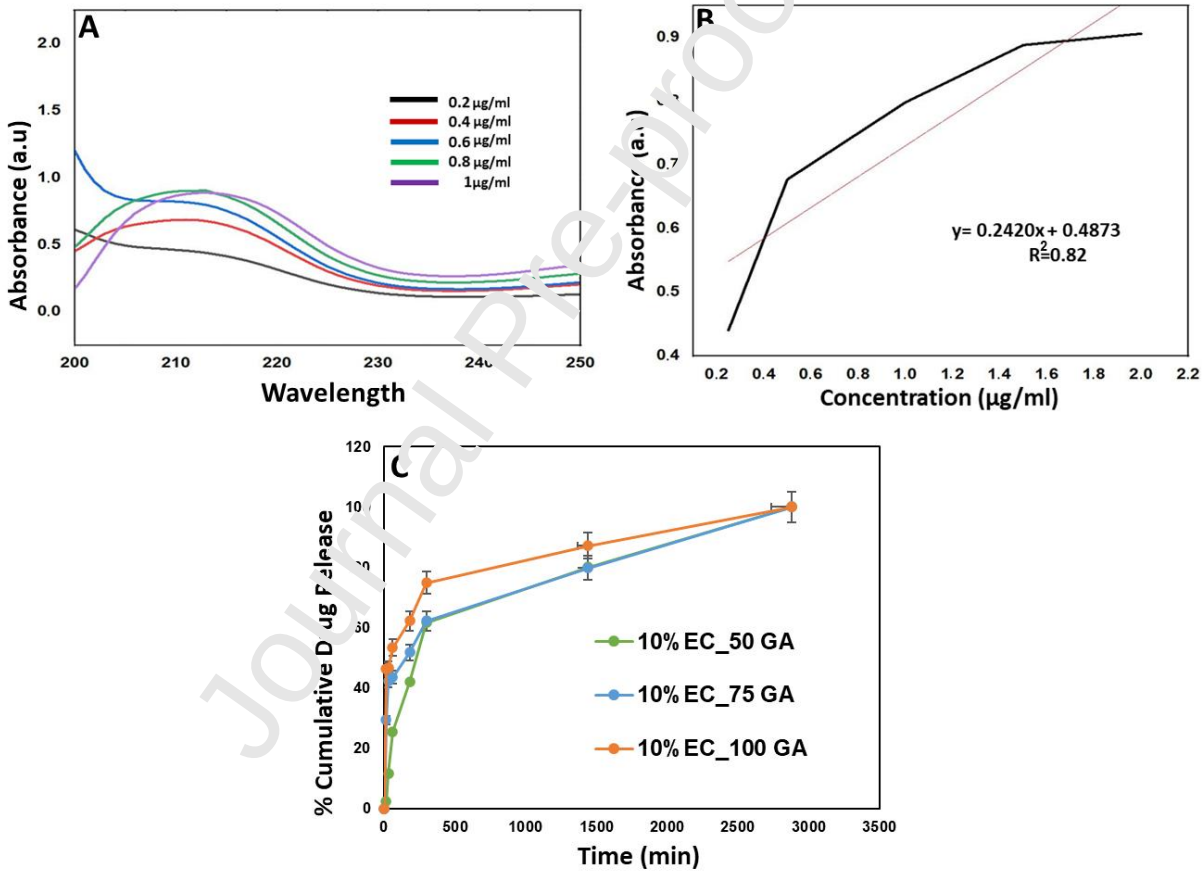

Figure 9. Calibration curve of the GA (**A**); absorbance graph obtained from calibration curve (**B**); the cumulative release graph of the three GA-loaded fibers (**C**).

Conclusions

In this study, novel 10%EC_GA fibers were successfully fabricated using the electrospinning technique. After inspection, the surface of the fibers displayed negligible changes in diameter,

indicating that the fiber structures were well-incorporated with consistent morphological properties. Comparing the average diameters of the GA-loaded fibers revealed a reduction in 10%EC fibers. The amount of GA released from the 10%EC fiber loaded with GA, when submerged in each medium, exhibited an initial rapid increase, followed by a relatively slower increase as the submersion time progressed. Moreover, the release behavior results demonstrated controlled and prolonged release of GA from 10%EC_100GA fiber, with the maximum release of the fibers being reached after 2 days. This behavior suggests that the release profile of GA from the fiber mats could be controlled and sustained, potentially offering benefits for wound healing applications. According to the MTT assay, GA-loaded fibers showed low cell viability on days 1 and 3 at lower concentrations, but also with the addition of a higher concentration of GA in these intervals, the cell viability increased. The 10%EC fibers loaded with GA presented significant antimicrobial efficacy, especially with variant 10%EC_100GA, which showed the potential for use as wound dressing materials. Our research shows that GA has potential therapeutic applications as an anti-inflammatory, indicating a > 90% microbial reduction capacity correlated with a logarithmic reduction ranging from 0.63 to 1. With regard to the morphological characteristic, the performance of the GA-loaded fibers can vary depending on the size of the fibers. GA will release more slowly from larger fibers because smaller molecules must first diffuse through larger fibers before they can be released. The mechanical characteristics of the GA-loaded fibers can also be influenced by the fiber size. Larger fibers have a tendency to make fibers stronger and more break-resistant. Given the imperative need for a pharmacokinetic equilibrium to be established between the release profile of GA and its rapid metabolic breakdown, the utilization of EC_GA fibers has been identified as a promising avenue for their application in the biomedical field, particularly as a viable material for wound dressing purposes. In addition, the biocompatibility properties of the EC_GA fibers should be reinforced for the usability of this combination to wound dressing applications.

Funding: We acknowledge the support of the UEFISCDI through PN-III-P2-2.1-PED-2019 project: "Evaluarea potentialului de exploatare a materialelor poroase in tratarea disbiozelor microbiotei" no. 524PED/2020. AMC ackowledge the support of UPB via the research grant "UPB—Proof of Concept 2020".

References

1. Desmet CM, Preat V, Gallez B. Nanomedicines and gene therapy for the delivery of growth factors to improve perfusion and oxygenation in wound healing. Adv Drug Deliver Rev. 2018;129:262-84.

2. Okur ME, Karantas ID, Senyigit Z, Okur NU, Siafaka PI. Recent trends on wound management: New therapeutic choices based on polymeric carriers. Asian J Pharm Sci. 2020;15(6):661-84.

3. Powers JG, Higham C, Broussard K, Phillips TJ. Wound healing and treating wounds Chronic wound care and management. J Am Acad Dermatol. 2016;74(4):607-25.

4. Goodarzi P, Alavi-Moghadam S, Sarvari M, Beik AT, Falahzadeh K, Aghayan H, et al. Adipose Tissue-Derived Stromal Cells for Wound Healing. Adv Exp Med Biol. 2018;1119:133-49.
5. Khalil H, Cullen M, Chambers H, Carroll M, Walker J. Elements affecting wound healing time: An evidence based analysis. Wound Repair Regen. 2015;23(4):550-6.
6. Karahan A, Abbasoglu A, Isik SA, Cevik B, Saltan C, Elbas NO, et al. Factors Affecting Wound Healing in Individuals With Pressure Ulcers: A Retrospective Study. Ostomy Wound Manag. 2018;64(2):32-9.
7. Moura LIF, Dias AMA, Carvalho E, de Sousa HC. Recent advances on the development of wound dressings for diabetic foot ulcer treatment-A review. Acta Biomater. 2013;9(7):7093-114.
8. Trevisol TC, Fritz ARM, de Souza SMAGU, Bierhalz ACK, Valle JAB. Alginate and carboxymethyl cellulose in monolayer and bilayer films as wound dressings: Effect of the polymer ratio. J Appl Polym Sci. 2019;136(3).
9. Tudoroiu E-E, Dinu-Pîrvu C-E, Albu Kaya MG, Popa L, Anuța V, Prisada RM, et al. An Overview of Cellulose Derivatives-Based Dressings for Wound-Healing Management. Pharmaceuticals. 2021;14(12):1215.
10. Wutticharoenmongkol P, Hannirojram P, Nuthong P. Gallic acid-loaded electrospun cellulose acetate nanofibers as potential wound dressing materials. Polym Adv Technol. 2019;30(4):1135-47.
11. Choi JS, Kim HS, Yoo HS. Electrospinning strategies of drug-incorporated nanofibrous mats for wound recovery. Drug Deliv Transl Re. 2015;5(2):137-45.
12. Seddiqi H, Oliaei E, Honarkar H, Jin JF, Geonzon LC, Bacabac RG, et al. Cellulose and its derivatives: towards biomedical applications. Cellulose. 2021;28(4):1893-931.
13. Yang D, Peng XW, Zhong LX, Cao XF, Chen W, Zhang XM, et al. "Green" films from renewable resources: Properties of epoxidized soybean oil plasticized ethyl cellulose films. Carbohyd Polym. 2014;103:198-206.
14. Oprea M, Voicu SI. Recent advances in composites based on cellulose derivatives for biomedical applications. Carbohyd Polym. 2020;247.
15. Vlaia L, Georgeta C, Olariu I, Vlaia V, Lupuleasa D. Cellulose-Derivatives-Based Hydrogels as Vehicles for Dermal and Transdermal Drug Delivery. 2016. p. 159-200.
16. Locatelli C, Filippin-Monteiro FB, Creczynski-Pasa TB. Alkyl esters of gallic acid as anticancer agents: A review. Eur J Med Chem. 2013;60:233-9.
17. Diaz-Gomez R, Lopez-Solis R, Obreque-Slier E, Toledo-Araya H. Comparative antibacterial effect of gallic acid and catechin against Helicobacter pylori. Lwt-Food Sci Technol. 2013;54(2):331-5.
18. Pinho E, Henriques M, Soares G. Cyclodextrin/cellulose hydrogel with gallic acid to prevent wound infection. Cellulose. 2014;21(6):4519-30.
19. Nguyen TTT, Ghosh C, Hwang SG, Tran LD, Park JS. Characteristics of curcumin-loaded poly (lactic acid) nanofibers for wound healing. J Mater Sci. 2013;48(20):7125-33.
20. Badhani B, Sharma N, Kakkar R. Gallic acid: a versatile antioxidant with promising therapeutic and industrial applications. Rsc Adv. 2015;5(35):27540-57.
21. Mohebian Z, Tajmohammadi I, Yavari Maroufi L, Ramezani S, Ghorbani M. A novel aloe vera-loaded ethylcellulose/hydroxypropyl methylcellulose nanofibrous mat designed for wound healing application. Journal of Polymers and the Environment. 2021:1-1.
22. Li HY, Zhang ZW, Godakanda VU, Chiu YJ, Angkawinitwong U, Patel K, et al. The effect of collection substrate on electrospun ciprofloxacin-loaded poly (vinylpyrrolidone) and ethyl cellulose nanofibers as potential wound dressing materials. Mat Sci Eng C-Mater. 2019;104.
23. M100 Performance Standards for Antimicrobial Susceptibility Testing A CLSI supplement for global application Available: www.clsi.orgAccessed: Mar. 30, 2022
24. Wang P, Li Y, Zhang C, Feng FQ, Zhang H. Sequential electrospinning of multilayer ethylcellulose/gelatin/ethylcellulose nanofibrous film for sustained release of curcumin. Food Chem. 2020;308.

25. Neo YP, Ray S, Jin J, Gizdavic-Nikolaidis M, Nieuwoudt MK, Liu DY, et al. Encapsulation of food grade antioxidant in natural biopolymer by electrospinning technique: A physicochemical study based on zein-gallic acid system. Food Chem. 2013;136(2):1013-21.
26. Singh D, Singh M. R. M, Semalty A, Semalty M: Gallic Acid-Phospholipid Complex: Drug Incorporation and Physicochemical Characterization, Letters in Drug Design & Discovery 2011; 8(3).27. Olga G, Styliani C, Ioannis RG. Coencapsulation of ferulic and gallic acid in hp-b-cyclodextrin. Food chemistry. 2015 Oct 15;185:33-40.
28. Trivedi MK, Branton A, Trivedi D, Nayak G, Mishra R, Jana S. Characterization of physicochemical and thermal properties of biofield treated ethyl cellulose and methyl cellulose. International Journal of Biomedical Materials Research. 2015 Dec 21;3(6):83-91.
29. Yu DG, Wang X, Li XY, Chian W, Li Y, Liao YZ. Electrospun biphasic drug release polyvinylpyrrolidone/ethyl cellulose core/sheath nanofibers. Acta Biomaterialia. 2013 Mar 1;9(3):5665-72.
30. Lu H, Wang Q, Li G, Qiu Y, Wei Q. Electrospun water-stable zein/ethyl cellulose composite nanofiber and its drug release properties. Materials Science and Engineering: C. 2017 May 1;74:86-93.
31. Minsart M, Van Vlierberghe S, Dubruel P, Mignon A. Commercial wound dressings for the treatment of exuding wounds: an in-depth physico-chemical comparative study. Burns & Trauma. 2022 Jan 1;10.
32. Tom IM, Ibrahim MM, Umoru AM, Umar JB, Bukar MA, Haruna AB, et al. Infection of Wounds by Potential Bacterial Pathogens and Their Resistogram. GALIL. 2019.
33. Maier S, Komer P, Diedrich S, Kramer A, Heidecke CD. Definition and management of wound infections. Chirurg. 2011;82(3):235-+.
34. Sisay M, Worku T, Edessa D. Microbial epidemiology and antimicrobial resistance patterns of wound infection in Ethiopia: a meta-analysis of laboratory-based cross-sectional studies. Bmc Pharmacol Toxico. 2019;20.
35. Bowler PG, Duerden BI, Armstrong DG. Wound microbiology and associated approaches to wound management. Clin Microbiol Rev. 2001;14(2):244-+.
36. Rashidi M, Mansour SS, Mostashari P, Ramezani S, Mohammadi M, Ghorbani M. Electrospun nanofiber based on Ethyl cellulose/Soy protein isolated integrated with bitter orange peel extract for antimicrobial and antioxidant active food packaging. Int J Biol Macromol. 2021;193:1313-23.
37. Li KJ, Guan GL, Zhu JX, Wu H, Sun QJ. Antibacterial activity and mechanism of a laccase-catalyzed chitosan-gallic acid derivative against Escherichia coli and Staphylococcus aureus. Food Control. 2019;96:234-43.
38. Sun XY, Dong MN, Guo ZK, Zhang H, Wang J, Jia P, et al. Multifunctional chitosan-copper-gallic acid based antibacterial nanocomposite wound dressing. Int J Biol Macromol. 2021;167:10-22.
39. Pinho E, Ferreira ICFR, Barros L, Carvalho AM, Soares G, Henriques M. Antibacterial Potential of Northeastern Portugal Wild Plant Extracts and Respective Phenolic Compounds. Biomed Res Int. 2014;2014.
40. Borges A, Ferreira C, Saavedra MJ, Simoes M. Antibacterial Activity and Mode of Action of Ferulic and Gallic Acids Against Pathogenic Bacteria. Microb Drug Resist. 2013;19(4):256-65.
41. Li ZJ, Liu M, Dawuti G, Dou Q, Ma Y, Liu HG, et al. Antifungal Activity of Gallic Acid In Vitro and In Vivo. Phytother Res. 2017;31(7):1039-45.
42. Kahkeshani N, Farzaei F, Fotouhi M, Alavi SS, Bahramsoltani R, Naseri R, et al. Pharmacological effects of gallic acid in health and diseases: A mechanistic review. Iran J Basic Med Sci. 2019;22(3):225-37.
43. Teodoro GR, Ellepola K, Seneviratne CJ, Koga-Ito CY. Potential Use of Phenolic Acids as Anti-Candida Agents: A Review. Front Microbiol. 2015;6.
44. Oh E, Jeon B. Synergistic anti-Campylobacter jejuni activity of fluoroquinolone and macrolide antibiotics with phenolic compounds. Front Microbiol. 2015;6.
45. Yang DJ, Moh SH, Son DH, You S, Kinyua AW, Ko CM, et al. Gallic Acid Promotes Wound Healing in Normal and Hyperglucidic Conditions. Molecules. 2016;21(7).

46. Rezaei-Seresht H, Cheshomi H, Falanji F, Movahedi-Motlagh F, Hashemian M, Mireskandari E. Cytotoxic activity of caffeic acid and gallic acid against MCF-7 human breast cancer cells: An in silico and in vitro study. Avicenna J Phytomedi. 2019;9(6):574-86.
47. Moghtaderi H, Sepehri H, Delphi L, Attari F. Gallic acid and curcumin induce cytotoxicity and apoptosis in human breast cancer cell MDA-MB-231. Bioimpacts. 2018;8(3):185-94.
48. Zhao B, Hu MC. Gallic acid reduces cell viability, proliferation, invasion and angiogenesis in human cervical cancer cells. Oncol Lett. 2013;6(6):1749-55.
49. Ahmadian S, Ghorbani M, Mahmoodzadeh F. Silver sulfadiazine-loaded electrospun ethyl cellulose/polylactic acid/collagen nanofibrous mats with antibacterial properties for wound healing. Int J Biol Macromol. 2020;162:1555-65.
50. Croitoru AM, Karacelebi Y, Saatcioglu E, Altan E, Ulag S, Aydogan HK, et al. Electrically Triggered Drug Delivery from Novel Electrospun Poly(Lactic Acid)/Graphene Oxide/Quercetin Fibrous Scaffolds for Wound Dressing Applications. Pharmaceutics. 2021;13(7).
51. Phiriyawirut M, Phaechamud T. Gallic Acid-loaded Cellulose Acetate Electrospun Nanofibers: Thermal Properties, Mechanical Properties, and Drug Release Behavior. Open Journal of Polymer Chemistry. 2012;2(1):21-9.
52. Petrisor G, Ficai D, Motelica L, Trusca RD, Birca AC, Vasile BS, et al. Mesoporous Silica Materials Loaded with Gallic Acid with Antimicrobial Potential. Nanomaterials-Basel. 2022;12(10).

Declaration of competing interest

The authors declare that they have no known competing financial interests or personal relationships that could have appeared to influence the work reported in this paper.